Observations of East Coast Upwelling Conditions in Synthetic Aperture Radar Imagery

Pablo Clemente-Colón and Xiao-Hai Yan, *Member, IEEE*

***Abstract*—Seasonal coastal upwelling in the U.S. Mid-Atlantic coastal ocean normally occurs during the summer months because of generally alongshore southerly wind episodes. Southerly winds force an offshore surface Ekman flow over the inner continental shelf. Colder and nutrient-rich waters from below upwell toward the surface replacing offshore-flowing surface waters. Synthetic Aperture Radar (SAR) observations from the European Remote Sensing (ERS) satellite ERS-2 before and after upwelling-favorable wind episodes in early summer 1996 along the New Jersey coast are presented here. Lower backscatter conditions appearing in the SAR imagery after the onset of upwelling demonstrate the influence of the upwelling regime on the sea surface roughness. Satellite sea surface temperature (SST) observations and *in-situ* sea temperature vertical profiles confirm upwelling conditions. Three key mechanisms are suggested to explain the lower radar returns observed under upwelling conditions, an increase in the atmospheric marine boundary layer stability, an increase in the viscosity of surface waters, and the presence of biogenic surfactants in the upwelling region.**

***Index Terms*—Coastal upwelling, ERS-2 SAR, ocean features, natural slicks, air-sea stability, sea surface backscatter.**

I. Introduction

SEASONAL coastal upwelling in the U.S. Mid-Atlantic coastal ocean normally occurs during the summer months because of generally alongshore southerly wind episodes [1]. Southerly winds along the U.S. East Coast can produce an offshore surface Ekman flow over the inner continental shelf. A divergent surface flow is compensated by an onshore deeper flow that brings colder and nutrient-rich water to the surface. If sustained, this process can become an important mechanism for cross-shelf exchanges in the region during summertime. In general, the duration and intensity of the wind events will determine the intensity and duration of the wind-driven flow. The Rossby radius of deformation and the horizontal gradient of the wind stress are important factors in determining the horizontal scale of the process [2].

Spaceborne instruments with infrared (IR) sensors, such as the NOAA Advanced Very High Resolution Radiometer (AVHRR), have been commonly used to detect upwelling activity by observing the contrast between colder upwelled waters and the surrounding warmer surface waters [3], [4]. Satellite visible sensors have been used to detect variations in ocean color associated with increased biological activity in upwelling regions [5], [6]. Cloud cover frequently limits the effectiveness of both IR and visible observations. Sun light availability imposes a further temporal constraint on visible observations. In contrast, an active satellite sensor such as the synthetic aperture radar (SAR) can be used day or night and under cloudy conditions to observe a variety of sea surface and coastal features of interest to oceanographers. These may include the signature of surface and internal waves, ocean currents and fronts, sea ice, bathymetry, and atmospheric phenomena [7]–[9]. In particular, certain regions of low radar return in SAR imagery (dark areas) are often attributed to the presence of upwelling, although in most cases, *in-situ* validation of the upwelling conditions is not provided. European Remote Sensing (ERS) satellite ERS-2 SAR observations acquired before and during confirmed upwelling conditions off the New Jersey coast are presented here.

Manuscript received November 9, 1998; revised June 7, 1999. This work is supported in part by the NOAA Ocean Remote Sensing (NORS) Program and the University of Delaware Sea Grant Office Program. ERS-2 SAR data was available through the CoastWatch Task of the National Ice Center AO2USA136 ESA Project.

P. Clemente-Colón is with NOAA/NESDIS/ORA E/RA3, NOAA Science Center, Camp Springs, MD 20746-4304 USA.

X.-H. Yan is with the Center for Remote Sensing, University of Delaware, Newark, DE 19716-3501 USA.

Publisher Item Identifier S 0196-2892(99)06967-3.

II. Low Backscatter Signatures in SAR Imagery

According to the theory of Bragg scattering, the SAR backscatter signal over the ocean is mainly due to resonance of the radar microwaves with capillary and short surface gravity waves of similar wavelength [10]. For a radar system with wavenumber k_r and an incidence angle θ, the main contributors to the backscattered radar energy are ocean waves with a wavenumber, k_b, given by

$$k_b = 2k_r \sin\theta. \tag{1}$$

The observed radar cross section return is proportional to the spectral density function of the so-called Bragg waves at this wavenumber. Wind generated Bragg waves provide the roughness elements required for the observation of most ocean features in SAR. As the roughness of the ocean surface increases, the backscatter power detected by the instrument increases. An increase in wind speed will thus result in an increase in radar return. Longer waves, surface currents, and atmospheric circulation processes can further modulate the Bragg wave spectrum. This modulation is required in order for SAR to image such ocean and ocean-atmosphere phenomena [11], [12].

In an upwelling dominated area, changes in the air stability at the boundary layer, due to changes in the air-sea temperature difference over upwelled waters, should have an important

effect on the observed backscatter [13]. Increased stability due to lower sea surface temperatures results in lower wind stress and thus a decrease in the spectral density of Bragg scattering waves. Furthermore, colder temperature of upwelled waters translates into important changes in the viscous properties of the surface layer. This in turn has an additional effect on the damping and initiation of Bragg waves and thus on the backscatter amplitude observed by SAR [14].

Natural and man-made surface slicks can be very effective in damping Bragg waves. Both of these produce very similar dark features in SAR imagery [15], [16]. Man-made slicks are commonly associated with the accidental spill or dumping of petroleum products (mineral slicks) as well as with the discharge of organic matter resulting from fishing activities. Natural slicks can also be mineral or biogenic in origin. Natural mineral slicks are commonly observed in areas dominated by ocean bottom oil seeps such as the Gulf of Mexico Green Canyon or the Santa Barbara Channel in Southern California. Biogenic slicks form because of higher concentrations of organic matter surface-active constituents of marine or terrigenous origin at the surface microlayer. Biogenic slicks may include lipids, proteins, organic acids, as well as many other complex molecules. Slick dominated areas in SAR imagery have been commonly associated with high biological activity [17].

The right wind speed conditions are required in order for slicks to form and be imaged by SAR. Under optimum wind speeds, accumulation along convergence zones and horizontal advection of slicks occurs and can serve as an indicator of the local circulation. At high wind speeds (7–8 m/s) significant background clutter develops. As soon as white-capping occurs, the observed effects of biogenic slicks become minimal [18]. As wind speed increases, slick-forming substances mix further down into the water column and become undetectable by SAR. On the other hand, if the wind speed is too low, the required contrast with the background is lost and the slicks become undetectable as well. In general, a minimum wind speed of 1–2 m/s is required to produce sufficient roughness for SAR imaging [19], [20]. Wind speed variations and rain also produce low backscatter signatures in SAR imagery. In fact, many low backscatter regions detected by SAR are simply the result of low local wind speeds. This creates problems in detecting and interpreting upwelling-induced low backscatter signatures.

III. Data Sources

Four ERS-2 SAR Precision digital image frames (SAR.PRI) of the New Jersey coastal region were provided by the European Space Agency (ESA). Two frames were acquired on May 29, 1996 around 15:43 UTC and two on June 14, 1996 around 15:40 UTC. ERS-2 is a multisensor satellite with a SAR mode Active Microwave Instrument (AMI) operating in the C-band (5.3 GHz) with VV-polarization and a nominal 23° fixed incidence angle at the center of the frame. SAR.PRI are 3-look images with a spatial resolution of 30 m along-track and 26.3 m across-track. The images have a swath width of 100 km and have been corrected for antenna elevation gain and spreading loss. Normalized radar cross sections (NRCS) in dB were calculated using the following expression:

$$\mathrm{NRCS} = 10\log 10(N^2 * (S * P + I)) \tag{2}$$

where N is the SAR.PRI data pixel value, P is the pixel number, and S and I are slope and intercept calibration parameters provided with each image.

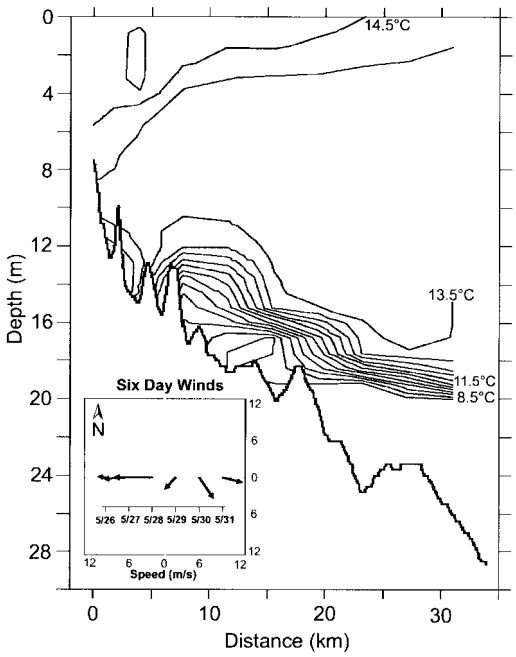

Fig. 1. CTD vertical profile of temperature obtained on May 31, 1996 along a cross-shelf line extending 30 km offshore from Little Egg Inlet. The plot indicates inshore deepening or downwelling of the surface layer isotherms. Daily mean wind vectors from May 26 to May 31 are shown in the inset box.

NOAA AVHRR visible and sea surface temperature (SST) images closest in time to the SAR observations were obtained from the National Oceanographic Data Center (NODC) CoastWatch archive. CoastWatch AVHRR images are mapped with a spatial resolution of about 1.42 km, about 50 times coarser than the SAR images. *In-situ* data were provided by the Rutgers University Institute of Marine and Coastal Sciences (IMCS) Remote Sensing Program. IMCS runs the LEO-15 observatory, a real-time observation network that includes an array of underwater instruments deployed offshore of Little Egg Inlet, north of Atlantic City, New Jersey [21]. CTD (Conductivity Temperature Depth sensor) temperature cross sections and wind observations were provided. The CTD data were collected on May 31 and June 12, 1996 along a cross-shelf transect extending 30 km offshore from Little Egg Inlet. Wind speed and direction were recorded at the IMCS Marine Field Station located close to the inlet.

IV. Observations During May 1996

A. Wind and SST Conditions by the End of May 1996

The recorded wind around the time of the May 29 SAR observations was a northeasterly wind of 4 m/s. A CTD vertical temperature profile obtained on May 31 along the Little Egg Inlet transect line shows inshore deepening of the

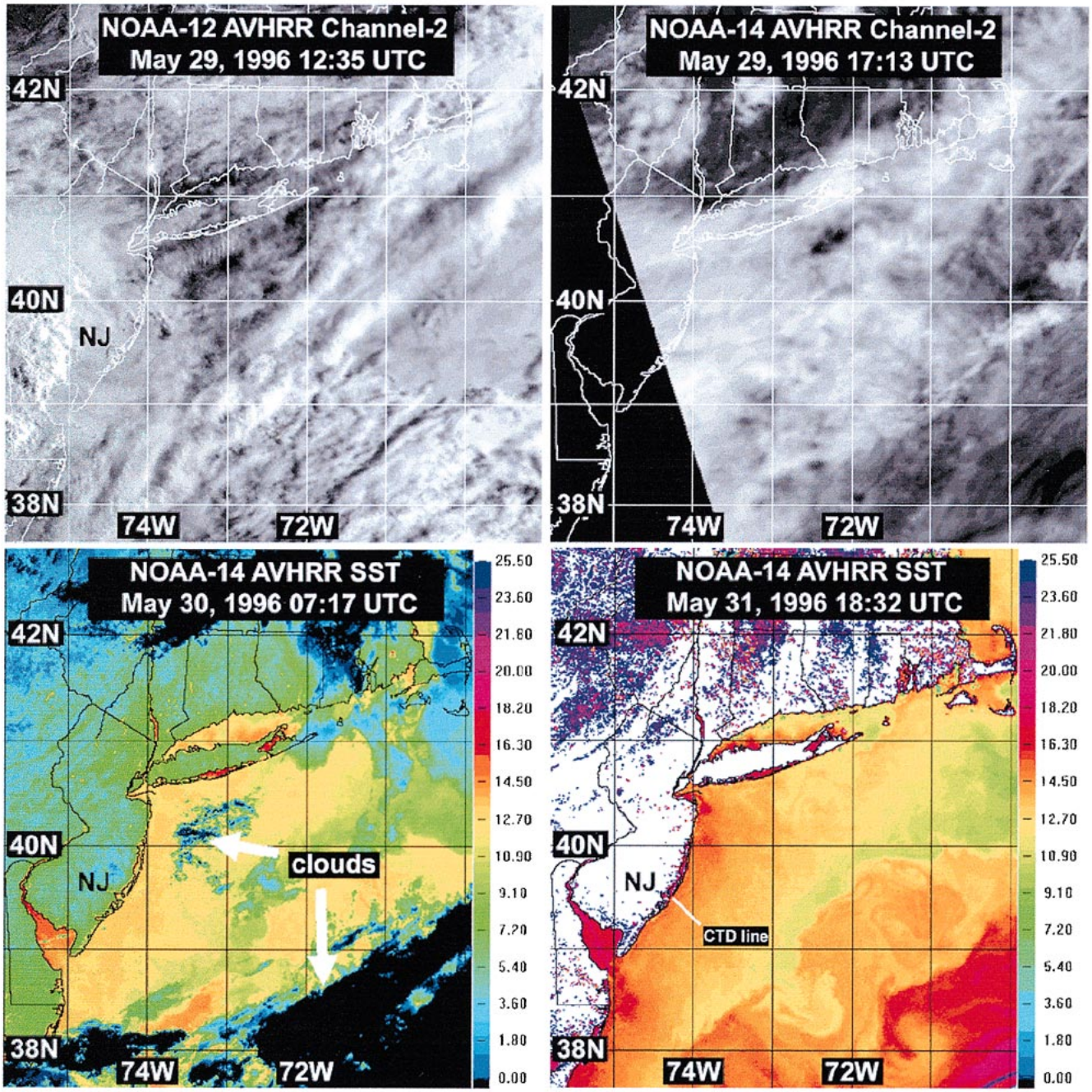

Fig. 2. NOAA AVHRR channel-2 visible (top) and SST (bottom) images from data acquired on May 29–31, 1996 over the Mid-Atlantic Bight. The visible images indicate complete cloud cover conditions on May 29. The SST images confirm homogeneous and relatively warm temperatures (compared to offshore conditions) off the New Jersey coast at the end of May.

isotherms and relatively uniform temperatures at the surface (Fig. 1). The mean direction of the winds during the six days leading to the CTD observations was not upwelling-favorable, i.e., did not have a southerly alongshore component. On the contrary, isotherm deepening is consistent with wind-forced downwelling. AVHRR data closest to the ERS-2 SAR acquisition time on May 29 indicate 100% cloud covered over the region as seen in the channel-2 images in Fig. 2. The first available cloud-free AVHRR SST images after the SAR pass are also shown in Fig. 2. The SST image for May 30 is from a nighttime pass. It indicates the presence of relatively uniform surface temperatures along the New Jersey coast. Colder offshore shelf waters as well as Gulf Stream warmer waters are also observed. Dark areas with bluish edges are due to cloud contamination. The SST image for May 31 is from a daytime pass. The location of the Little Egg Inlet CTD transect line is indicated on the image. Slightly higher temperatures are shown along the coast. This is likely due to diurnal heating. Again, relatively homogeneous SST conditions along the coast are observed. Both, the CTD and AVHRR SST observations, provide clear and convincing evidence of the absence of an upwelling regime in the region at the end of May 1996.

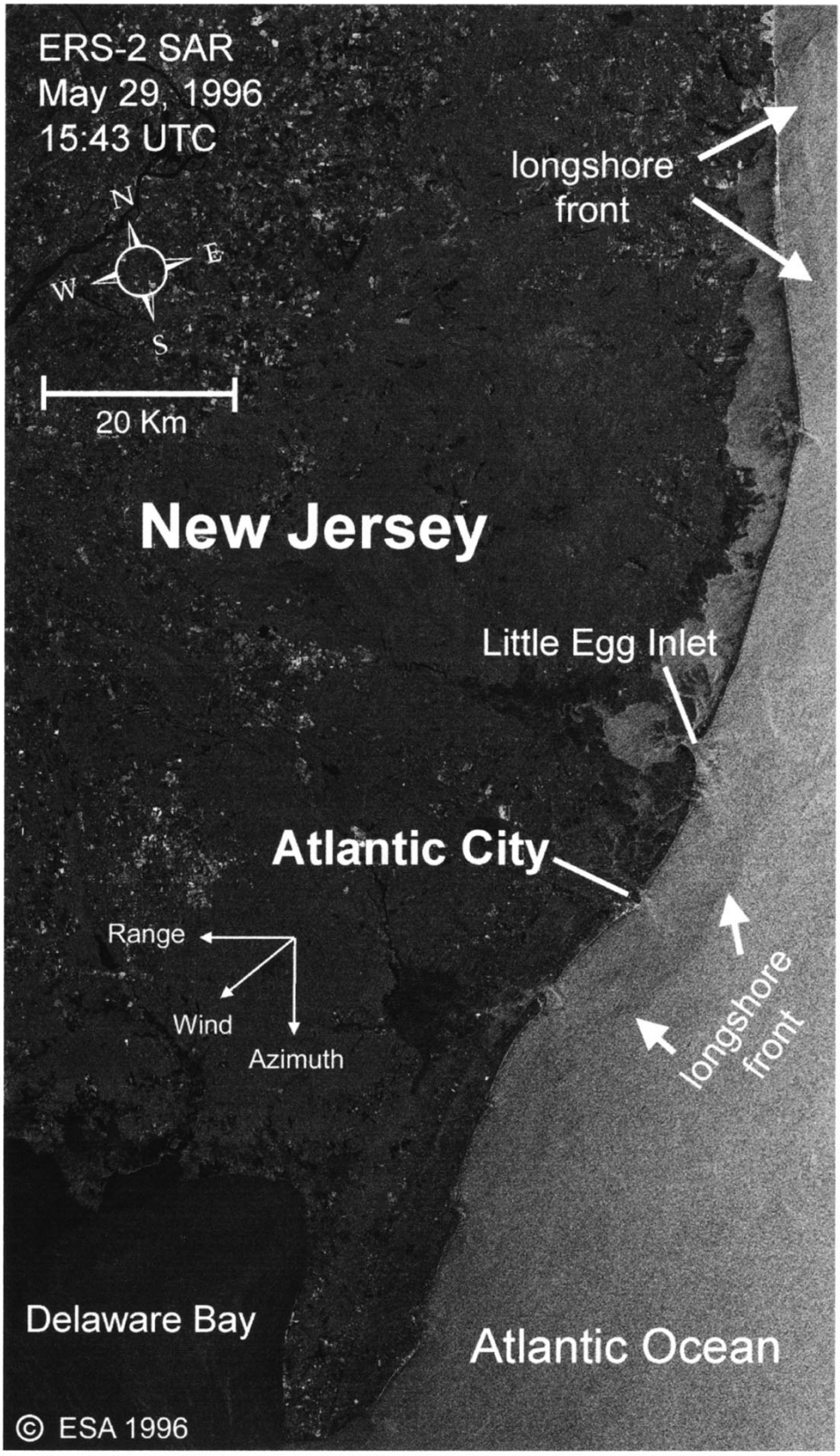

Fig. 3. ERS-2 SAR image acquired on May 29, 1996 at 15:43 UTC over the New Jersey coastal region. The image shows relatively homogenous backscatter conditions over the ocean, outflow signatures from several inlets, and a faint indication of a longshore front.

B. SAR Surface Conditions on May 29

The two ERS-2 SAR.PRI image frames acquired on May 29, 1996 at about 15 : 43 UTC over the New Jersey coast were combined. A subimage centered on the Little Egg Inlet region is shown in Fig. 3. Unfortunately, limited coverage of the shelf region to the north is provided by this image. A very uniform radar return is observed over the coastal ocean. A very uniform radar return with relatively high mean NRCS of the order of -5 dB ± 2 dB is observed over the coastal ocean. Under closer examination, the image shows some indications of tidal plumes from inlets (slightly brighter features). In addition, a slightly darker inshore region weakly delineates a long frontal feature along the coast. This feature is probably associated with a northerly coastal buoyant flow from the Hudson River Estuary. Again, it should be pointed out that these SAR observations were obtained under 100% cloud cover conditions.

V. Observations During June 1996

A. Wind and SST Conditions by Mid-June 1996

Persistent upwelling-favorable southerly winds were recorded in the New Jersey coastal region during the second week of June 1996. The wind around the time of the ERS-2 SAR pass on June 14 was a southeasterly of 3.3 m/s. A CTD vertical temperature profile obtained on June 12 (Fig. 4) indicates shoaling of the isotherms toward the coast and colder surface waters inshore. These upwelling conditions were set by southerly winds that blew over the region during the six days leading to the CTD observations. AVHRR SST images available for June 14 were cloud contaminated and are not shown. Fortunately, AVHRR SST data for June 12 and 13 (Fig. 5) captured regions of colder SST developed along the New Jersey coast, the Delaware Bay mouth and the Delaware coast. The observed SST distribution is consistent with the seasonal development of coastal upwelling centers along the Mid-Atlantic Bight [1]. Also, consistent with available *in-situ* observations, a minimum satellite SST of around 16 °C was found in the upwelling region. Sample AVHRR SST plots along line A (coincident with the CTD line) and line B shown on the June 13 SST image (Fig. 5) are included at the bottom of Fig. 7. On the average, the cross-shelf SST gradient off the coast of New Jersey is estimated to be of the order of 0.15°C /km on June 13.

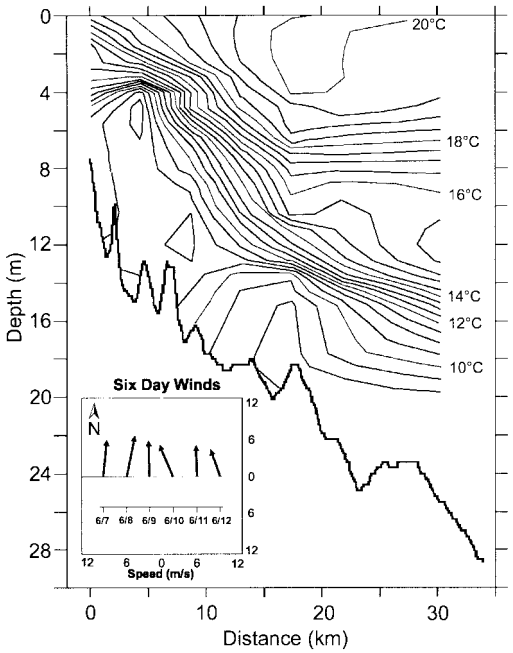

Fig. 4. CTD vertical profile of temperature obtained on June 12, 1996 along a cross-shelf line extending 30 km offshore from Little Egg Inlet. The plot indicates inshore upwelling of the surface layer isotherms. Upwelling-favorable daily mean wind vectors from June 7 to June 12 are shown in the inset box.

B. SAR Surface Conditions on June 14

The two ERS-2 SAR.PRI image frames acquired on June 14, 1996 at about 15 : 40 UTC were combined and a subimage is shown in Fig. 6. Surface conditions greatly differ from those observed on the May 29 image. The inner shelf region off the New Jersey coast is now dominated by significantly lower radar backscatter. Several regions of extreme low backscatter and the abundance of filaments or slick features along the coast are now observed. NRCS 50-pixel averaged values along cross-track sample lines on the June 14 SAR image are shown in Fig. 7. NRCS offshore values are at the same level, around -5 dB, as those found inshore on May 29. This is interesting since offshore temperatures by mid-June were higher than inshore temperatures at the end of May. Furthermore, this observation cannot be explained by the NRCS dependence on the incidence angle since both the June 14 offshore region and the May 29 inshore region are in the near range of the SAR swath and were thus imaged at about the same incidence angle. The most likely explanation is that the increase in backscatter expected as a result of higher SST (lower stability) on June 14 has been countered by a decrease resulting from the lower wind speed observed at the time. More importantly, the mean June 14 NRCS values uniformly decrease from the -5 dB level offshore to about -15 dB inshore, with even much lower values found over slick features. Over slick-free areas, the data show an overall cross-track backscatter attenuation gradient of around 0.14–0.2 dB/km. For winds from 2–4 m/s, the NRCS dependence on the incidence angle for C-band VV-polarization translates into a ratio of less than 0.06 dB/km [22]. Subtracting this amount from our estimated attenuation gradient results in a backscatter attenuation of about 0.08–0.14 dB/km that can be attributed to the modulation caused by the upwelling regime.

VI. Discussion

From the SAR observations presented above, lower backscatter and the presence of filaments or slick features over the New Jersey inner shelf region appear to be associated with the onset of a coastal upwelling regime. The relatively homogeneous backscatter conditions observed by SAR on May 29 reflect the homogeneous AVHRR SST conditions observed shortly after. AVHRR and CTD observations indicate the absence of upwelling conditions by the end of May. In contrast, SAR backscatter on June 14 decreases rapidly from the outer shelf to the inner shelf region where the coldest waters were observed less than a day earlier. Both, lower

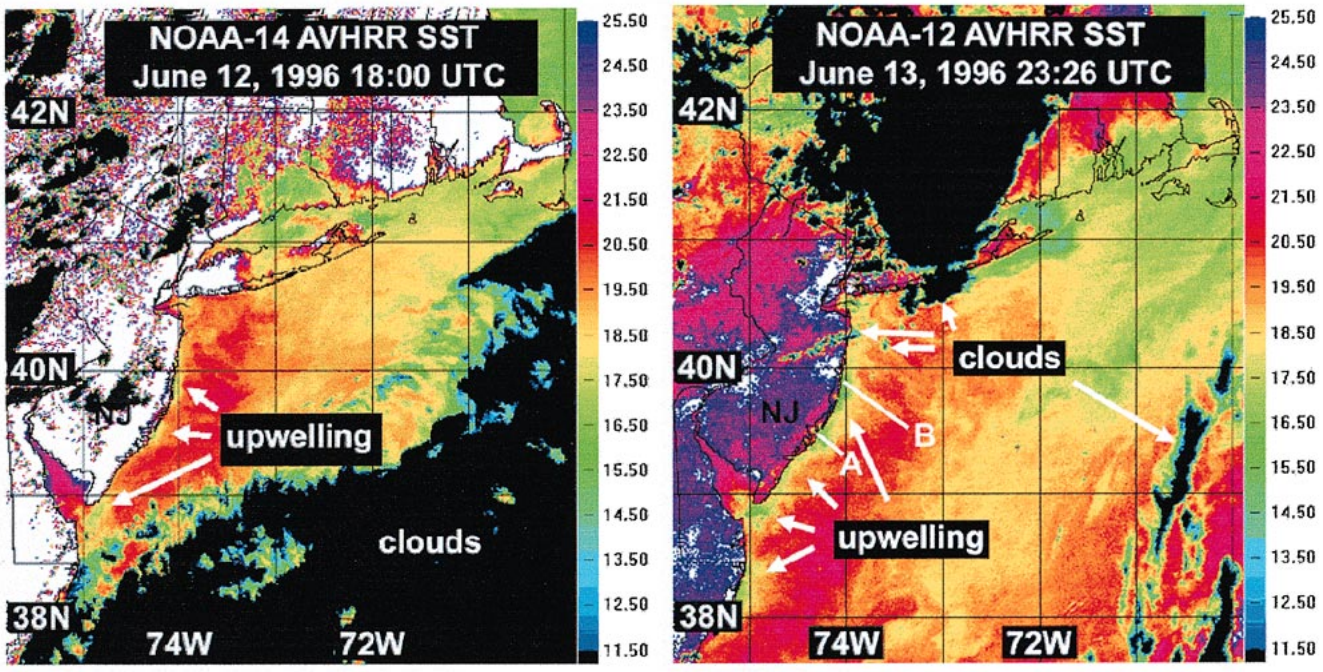

Fig. 5. NOAA AVHRR SST images from data acquired on June 12–13, 1996 over the Mid-Atlantic Bight. The images show active upwelling along the New Jersey coast. SST transect lines A and B on June 13 were placed across upwelling centers and are plotted in Fig. 7.

wind stress resulting from increased stability and damping of capillary waves resulting from increased viscosity must play a role in producing the observed offshore-inshore backscatter attenuation gradient in the SAR imagery during upwelling conditions. It is well known that changes in sea surface temperature can in fact produce significant changes in radar backscatter [8], [13], [23]. The air-sea boundary layer stability is a function of the air-sea temperature difference. Stability changes produce changes in the turbulent flow over the sea surface. Lower SST increases stability and decreases turbulence, which in turn results in lower wind stress. Consequently, the generation of Bragg waves is reduced and a lower radar return should be observed over colder waters. Radar backscatter has also been shown to depend on water temperature through changes in water viscosity. Lower temperature increases water viscosity. Increased viscosity produces increased damping and affects the initiation of Bragg waves, which also results in lower radar return [14]. The effect of changes in surface tension and dielectric constant with temperature are less significant than those caused by stability or viscosity changes.

The distribution of SST associated with the localized seasonal upwelling in the Mid-Atlantic Bight is clearly detectable using AVHRR notwithstanding the low spatial resolution of the sensor. Combining the SAR NRCS attenuation gradient estimate for June 14 and the mean AVHRR SST gradient observed on June 13, a ratio can be computed to provide a crude estimate of backscatter sensitivity on temperature over the upwelling region. A backscatter to SST ratio of approximately 0.5–1.0 dB/°C is obtained.

Our ability to observe natural slicks can provide an important link between the wind physical forcing and the biological activity of the ocean. The high spatial resolution of the SAR data allows for natural slick filaments to be imaged over a highly productive upwelling area. In an upwelling regime, the presence of natural biogenic slick filaments serves as an indicator of the enhanced productivity resulting from the high-nutrient water environment. The slick patterns on the June 14 SAR image are characterized by drastic drops in backscatter relative to the offshore-inshore gradient, in some cases all the way down to the noise-floor of the sensor (see line c in Fig. 7). We did not find any similarly drastic reductions in the AVHRR SST over those areas most heavily dominated by slicks in the SAR image. Of course, higher resolution SST data are probably required to convincingly show this. Nevertheless, the present observations suggest that, when present, slicks are likely to be a more important factor in reducing the local backscatter than temperature changes. In slick free areas, the next most likely mechanism for backscatter reduction is, in our opinion, increased stability over colder upwelled waters. Unfortunately, water viscosity and stability effects on backscatter occur simultaneously in the real world and it is not clear if their relative contributions can be separated from each other in field observations. Based on X-band laboratory water tank measurements, Zheng *et al.* [14] proposed a semi-analytic model to relate the effect of surface temperature on backscatter, due to changes in water viscosity, as follows:

$$\Delta\sigma_o = 0.24\Delta T \tag{3}$$

where $\Delta\sigma_o$ is the change in NRCS in dB and ΔT is the change in surface temperature in °C. If we assume this relation also holds for C-band, we can subtract 0.24 dB/°C from our estimate of backscatter to SST ratio and would obtain a stability dependence on temperature of the order of 0.26–0.76 dB/°C.

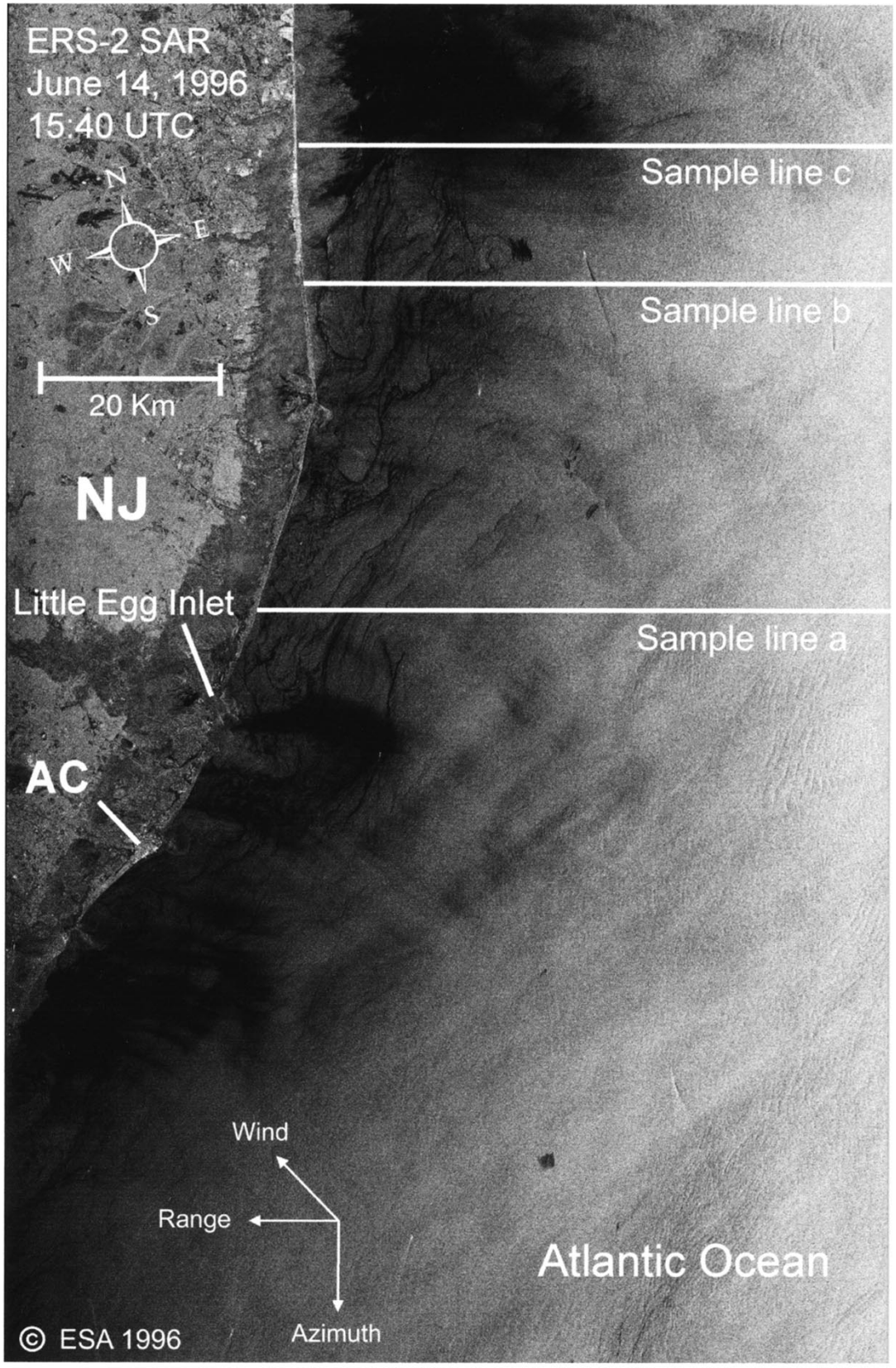

Fig. 6. ERS-2 SAR image acquired on June 14, 1996 at 15 : 40 UTC over the New Jersey coastal region. The image shows significant reduction of inshore backscatter and an abundance of slick filaments along the coast in contrast with the May 29 conditions. NRCS along selected sample lines a, b, and c is plotted in Fig. 7.

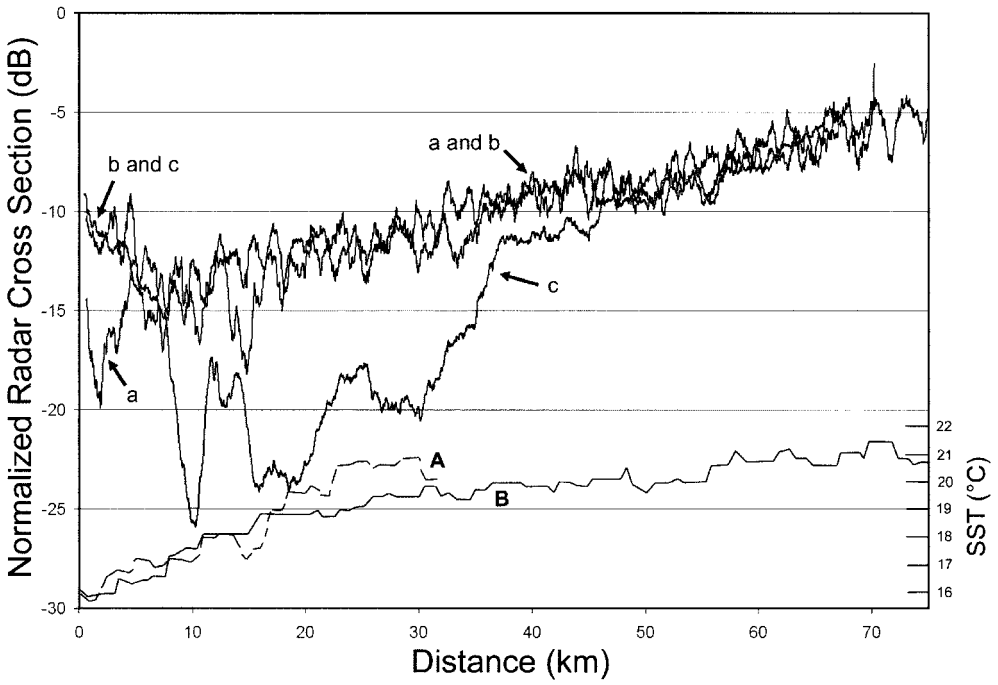

Fig. 7. Mean NRCS plot along the cross-track sample lines a, b, and c on the June 14, 1996 SAR image. The plot for line c indicates the overwhelming effect of slicks and possibly local low wind features on the radar return. SST along transects lines A and B on the June 13, 1996 AVHRR SST image (Fig. 5) is plotted at the bottom.

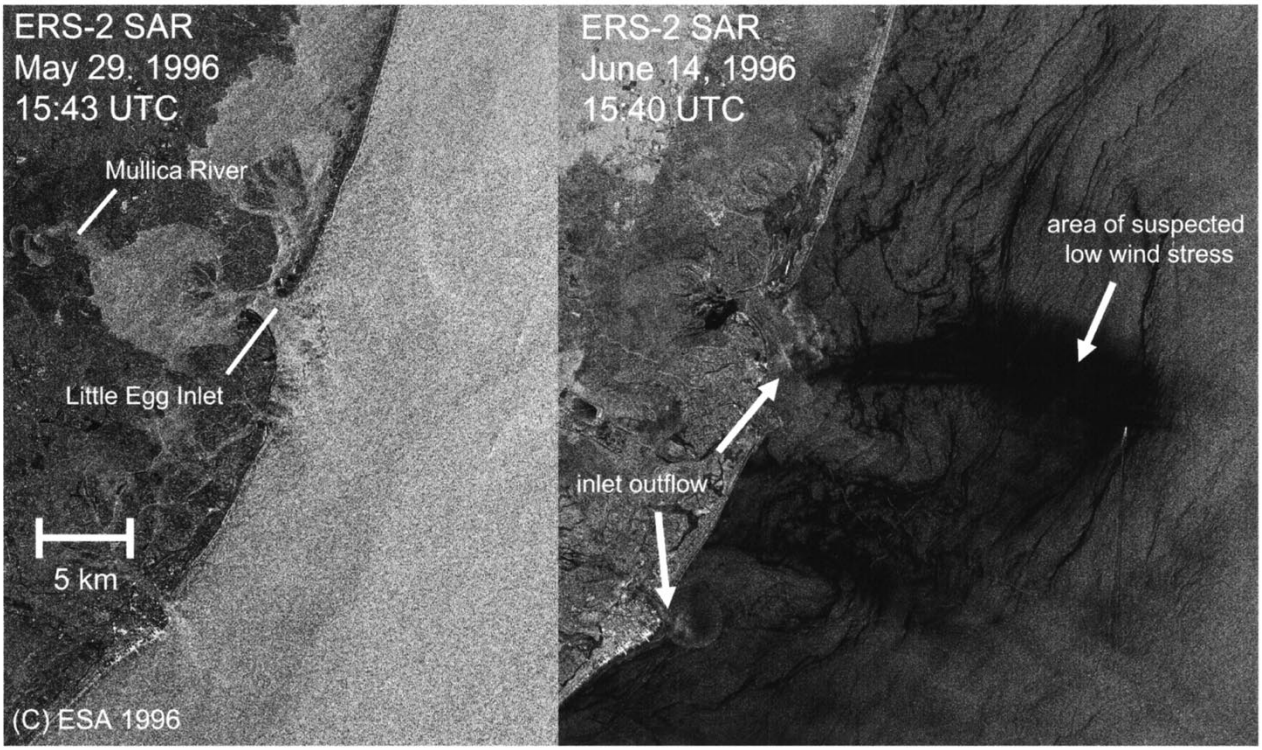

Fig. 8. ERS-2 SAR close-ups of the Little Egg Inlet region on May 29 and June 14, 1996 showing indications of inlet outflow, slicks, and low wind speed features.

It is interesting that the location and shape of a low backscatter feature found off Little Egg Inlet on June 14 appeared to match at first that of a cold cyclonic eddy observed in surface current data acquired by IMCS and delineated by the SST. This location has been historically identified as one of the recurring seasonal upwelling centers. Closer examination of the SAR image at a higher spatial resolution (Fig. 8) reveals a combination of two separate patterns, neither of which necessarily correlates with the surface current observations. One side of the feature (lower part) is actually dominated by a

dense concentration of slicks while the other side (upper part) appears to be an unrelated wind stress variability-like pattern (soft edges). While lower wind stress is consistent with colder temperatures, the slick pattern itself does not trace the cyclonic surface circulation of an eddy as originally suspected. At the time of the SAR pass, Little Egg Inlet was at an early midway ebb stage. This inlet provides outflow to the Mullica River, the major drainage system along the New Jersey coast. It is plausible that the formation of the slick pattern is related to surfactant outflow through the inlet or that it may result from the impact of the inlet plume circulation on the distribution of shelf-produced slicks. The fact is that ubiquitous slick features are observed along the full length of the coast on June 14 while no evidence of slicks is present on the May SAR image when the tide was at maximum ebb. This reinforces our belief that the slick patterns observed on June 14 along the New Jersey coast are for the most the result of biological enhancement due to the prevailing upwelling activity in the region.

A second low backscatter feature of interest was observed to the north (top of Fig. 6), just south of the Hudson River Estuary. This feature also coincides with the location of another of the known recurrent upwelling centers. The feature appears to be somehow "detached" from the coast. High outflow from the Hudson River was actually reported during the month of June [24]. The apparent detachment of this feature from the coast may be an indication of the interaction between the coastal buoyant flow imposed by the Hudson River Estuary discharge and the upwelling processes taking place over the shelf.

It is evident that the interpretation of SAR imagery without any ancillary information is difficult. For example, the observed reduction in backscatter on June 14, attributed to upwelling conditions, may have been misinterpreted instead as resulting from wind variability effects had no SST information been available. Clearly, SAR observations can provide substantially better and less ambiguous information when combined with other remote sensing and *in-situ* data.

VII. Conclusions and Future Work

The data presented above have shown for the first time the occurrence of SAR low backscatter features associated with confirmed seasonal upwelling activity on the New Jersey inner shelf area. The decrease in radar return coincided with the presence of an upwelling regime. The backscatter sensitivity on temperature over the upwelling region was estimated to be of the order of 0.5–1.0 dB/°C. Unfortunately, simultaneous observations of local wind speed and direction, air and sea surface temperature, and even biological microlayer sampling will be required in order to better quantify the contribution of key mechanism producing the SAR signature These mechanisms include changes in the air-sea stability, changes in the viscous properties of seawater, and the surface layer accretion of biological surfactants. A backscatter model containing parameters for wind speed, air-sea stability, viscosity dependence on SST, and the presence of organic constituents at the surface needs to be developed. As shown by the SAR data, the New Jersey coastal ocean was characterized by the prevalence of slicks of suspected natural origin on June 14. The observed abundance of slick filaments in the area suggests high biological activity which results from increased nutrient availability in the euphotic zone produced by sustained upwelling. *In-situ* verification of the nature of the slicks is still required.

These observations show the potential of SAR data observations for studying and monitoring the onset and evolution of upwelling in coastal regions. These observations encouraged a follow-up study that is testing the recurrence of seasonal upwelling signatures as seen by SAR in the Mid-Atlantic Bight. A verification experiment was carried out in coordination with the IMCS upwelling observation program during May through July 1998. The research addresses the effects of observed circulation and environmental conditions on the appearance, location, and morphology of SAR features generated by the summer upwelling activity. Close to 100 SAR images from the Canadian Space Agency's RADARSAT satellite and from ERS-2 collected during summer 1998 off the U.S. East Coast are now available. Continuos wind temperature, and current *in-situ* datasets, as well as AVHRR and ocean color observations from the SeaWiFS satellite are also available. A preliminary assessment of the data has revealed once again significant contrast between backscatter conditions off the coast of New Jersey before, during and after confirmed upwelling episodes.

Acknowledgment

The authors would like to acknowledge the ongoing collaboration on this research with S. Glenn, R. Chant, and M. Crawly of IMCS at Rutgers University, as well as the useful suggestions and comments from Dr. Q. Zheng, UDEL, and Dr. L. C. Breaker, NWS.

References

[1] S. M. Glenn, M. F. Crowley, D. B. Haidvogel, and Y. T. Song, "Underwater observatory captures coastal upwelling events off New Jersey," *EOS Trans. AGU*, vol. 77, no. 25. pp. 233–236, June, 1996.

[2] G. A. Dalu and R. A. Pielke, "An analytical study of the frictional response of coastal currents and upwelling to wind stress," *J. Geophys. Res.*, vol. 95, pp. 1523–153, 1990.

[3] A. P. Cracknell, Ed., *Space Oceanography*. Singapore: World Scientific, 1992.

[4] J. J. Bisagni and M. H. Sano, "Satellite observations of sea surface temperature variability on southern Georges Bank," *Cont. Shelf Res.*, vol. 13, pp. 1045–1064, 1993.

[5] C. R., McClain, L. J. Pietrafesa, and J. A. Yoder. "Observations of gulf stream-induced and wind-driven upwelling in the Georgia bight using ocean color and infra-red imagery," *J. Geophys. Res.*, vol. 89, pp. 3705–3723, 1984.

[6] F. M. Sousa and A. Bricaud, "Satellite-derived phytoplankton pigment structures in the Portuguese upwelling area," *J. Geophys. Res.*, vol. 97, pp. 11,343–11,356, 1992.

[7] R. Beal, V. Kudryavtsev, D. Thompson, S. Grodsky, D. Tilley, and V. Dulov, "Large and small scale circulation signatures of the ERS-1 SAR over the Gulf Stream," in *Proc. 2nd ERS-1 Symp.*, Hamburg, Germany, Oct. 11–14, 1993, ESA SP-361, pp. 547–552, 1994.

[8] C. S. Nilsson and P. C. Tildesley, "Imaging of oceanic features by ERS 1 synthetic aperture radar," *J. Geophys. Res.*, vol. 100, no. C1, pp. 953–967, 1995.

[9] D. L. Evans, Ed., *Spaceborne Synthetic Aperture Radar: Current Status and Future Directions. A Report to the Committee on Earth Sciences*, Space Studies Board, National Research Council, NASA Tech. Memo., pp. 4679, Apr. 1995.

[10] G. R. Valenzuela, "Theories for the interaction of electromagnetic and ocean waves—A review," *Boundary-Layer Meteorol.*, vol. 13, pp. 61–85, 1978.
[11] G. O., Marmorino, D. R. Thompson, H. C. Graber, and C. L. Trump, "Correlation of oceanographic signatures appearing in synthetic aperture radar and interferometric aperture radar imagery with *in situ* measurements," *J. Geophys. Res.*, vol. 102, pp. 18,723–18,736, 1997.
[12] Q. Zheng, X.-H. Yan, C.-R. Ho, V. Klemas, Z. Wang, and N.-J. Kuo, "Coastal lee waves on ERS-1 SAR images," *J. Geophys. Res.*, vol. 103, no. C4, pp. 7,979–7,993, 1998.
[13] C. A. Friehe, W. J. Shaw, D. P. Rogers, K. L. Davidson, W. G. Large, S. A. Stage, G. H. Crescenti, S. J. S. Khalsa, G. H. Greenhunt, and F. Li, "Air-sea fluxes and surface layer turbulence around a sea surface temperature front," *J. Geophys. Res.*, vol. 96, pp. 8593–8609, 1991.
[14] Q. Zheng, X.-H. Yan, N. E. Huang, V. Klemas, and J. Pan, "The effects of water temperature on radar scattering from the water surface: An X-band laboratory study," *The Global Atmos. Ocean Syst.*, vol. 5, pp. 273–294, 1997.
[15] W. Alpers and H. Hühnerfuss, "The damping of ocean waves by surface films: A new look at an old problem," *J. Geophys. Res.*, vol. 94, pp. 6251–6265, 1989.
[16] M. Gade, W. Alpers, H. H. Huhnerfuss, V. R. Wismann, and P. A. Lange, "On the reduction of the radar backscatter by oceanic surface films: Scatterometer measurements and their theoretical interpretation," *Remote Sens. Environ.*, vol. 66, no. 1, pp. 52–70, Oct. 1998.
[17] H. A. Espedal, O. M. Johannessen, and J. C. Knulst, "Satellite detection of natural films on the ocean surface," in *Geophys. Res. Lett.*, vol. 23, pp. 3,151–3,154, 1996.
[18] J. R. Apel, R. F. Gasparovic, D. R. Thompson, and B. L. Gotwols, "Signatures of surface wave/internal wave interactions: Experiment and theory," *Dynam. Atmos. Oceans*, vol. 2, pp. 89–106, 1996.
[19] R. F. Gasparovic, J. R. Apel, D. R. Thompson, and J. S. Tochko, "A comparison of SIR-B synthetic aperture radar data with ocean internal wave measurements," *Science*, vol. 232, pp. 1529–1531, 1986.
[20] J. Vogelzang, G. J. Wensink, G. P. de Loor, H. C. Peters, and H. Pouwels, "Sea bottom topography with X band SLAR: The relation between radar imagery and bathymetry," *Int. J. Remote Sensing*, vol. 13, pp. 1,943–1,958, 1992.
[21] S. M. Glenn, D. B. Haidvogel, O. M. E. Schofield, C. J. von Alt, and E. R. Levine, "Coastal predictive skill experiments. A Littoral Laboratory, data-assimilative forecast model linked to adaptive multiplatform network being evaluated," *Sea Tech.*, vol. 39, no. 4, pp. 63–69, Apr. 1998.
[22] A. Skøelv, S. T. Dokken, and T. Wahl, "Up-coming radar satellites and their potential for some maritime applications," in *Progress in Environmental Remote Sensing Research and Applications*, E. Parlow, Ed. Rotterdam, The Netherlands: Balkema, 1996, pp. 301–307.
[23] D. P. Rogers, D. W., Johnson, and C. A. Friehe, "The Stable internal boundary layer over a coastal sea—Airborne measurements of the mean and turbulence structure," *J. Atmos. Sci.*, vol. 52, no. 6, pp. 667–683, 1995.
[24] R. Chant, personal communication, IMCS, Rutgers Univ., Piscataway, NJ, 1997.

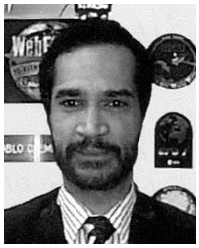

Pablo Clemente-Colón received the B.S. degree in physics from the University of Puerto Rico, Mayagüez, in 1977 and the M.S. degree in oceanography from Texas A&M University, College Station, in 1980. He is currently pursuing the Ph.D. degree in ocean remote sensing at the University of Delaware, Newark.

He is an Oceanographer at the National Environmental Satellite, Data, and Information Service (NESDIS) Office of Research and Applications, National Oceanic and Atmospheric Administration (NOAA), Camp Springs, MD, since 1980. His research interests include satellite oceanography, operational sea surface temperature monitoring, synthetic aperture radar coastal applications, upper ocean dynamics, ocean color, remote sensing fisheries, marine boundary processes, and data fusion.

Xiao-Hai Yan (M'93) received the B.S. (equiv.) degree in marine science in 1977 from Tongchi University, Shanghai, China. In 1989, he received the Ph.D. degree in physical and satellite oceanography from the State University of New York at Stony Brook.

From 1977 to 1985, he held a research scientist position in the Shanghai Institute of Technical Physics, Academia Sinica, China. He was a Postdoctoral Research Associate, Scripps Institution of Oceanography, University of California, San Diego, from 1989 to 1990. From 1990 to 1993, he was an Assistant Professor and is currently a Professor and Associate Director in the Center for Remote Sensing, College of Marine Studies, University of Delaware, Newark. His teaching and research are primarily in the areas of remote sensing, image processing, and satellite oceanography. He has been a principal investigator for National Science Foundation, NASA, NOAA, and the Office of Naval Research for Ocean Remote Sensing.

Dr. Yan is a member of AGU, the American Meteorological Society, the Oceanography Society, and IGARS. He is also a National Science Foundation Presidential Faculty Fellow.